Available online at www.sciencedirect.com
SCIENCE DIRECT
Sensors and Actuators A 130–131 (2006) 531–536
SENSORS AND ACTUATORS A PHYSICAL
www.elsevier.com/locate/sna

Study on a PZT-actuated diaphragm pump for air supply for micro fuel cells

Xing Yang [a,b,c,*], Zhaoying Zhou [a,b,c], Hyejung Cho [d], Xiaobing Luo [d]

[a] *MEMS Lab, Department of Precision Instruments & Mechanology, Room 4301, Tsinghua University, Beijing 100084, PR China*
[b] *Micro-Nano Technology Research Center, Tsinghua University, Beijing 100084, PR China*
[c] *State Key Laboratory of Precision Measurement Technology and Instruments, Tsinghua University, Beijing 100084, PR China*
[d] *Samsung Advanced Institute of Technology, Suwon 440-600, South Korea*

Received 4 June 2005; received in revised form 10 November 2005; accepted 2 December 2005
Available online 20 January 2006

Abstract

This paper presents a micro diaphragm air pump actuated by PZT bimorphs for air supply for micro fuel cells. The pump is characterized by thin structure, large air flow rate, low power consumption, etc. A prototype of the micro diaphragm air pump, with a size of 60 mm × 16 mm × 2 mm, was fabricated by precise manufacturing. Simulations and experiments showed that the diaphragm air pump has high efficiency and good performance. With a voltage of 20 V, the air pump's flow rate is 85.3 ml/min (the flow velocity is about 0.2 m/s) in resonance and its power consumption is only 3.18 mW.

Keywords: Micro gas pump; Bimorph; Air supply; Diaphragm; Micro fuel cell

1. Introduction

A fuel cell is a kind of electrochemical device that converts the chemical energy of reactants directly into electricity, which offers advantages of high energy density, low volume and weight, no moving parts and no harmful emissions. Recently, miniature fuel cells have been drawing increasing attention as a possible solution to the search for improved power sources for portable power systems [1].

The direct methanol fuel cell (DMFC) is one of the fuel cells which have the potential to be miniaturized. The chemical reaction in DMFC is as follows:

$$\text{Anode}: \ CH_3OH + H_2O \rightarrow CO_2 + 6H^+ + 6e^-$$

$$\text{Cathode}: \ \tfrac{3}{2}O_2 + 6H^+ + 6e^- \rightarrow 3H_2O$$

$$\text{Overall reaction}: \ CH_3OH + \tfrac{3}{2}O_2 \rightarrow CO_2 + 2H_2O$$

From the equation above, it holds true that in a completely passive system, the entire surface area of the fuel cell cathode must be exposed to the exterior to allow air to reach the catalyst layer. For longer durations, however, in the absence of convection, the local oxygen concentration adjacent to the cathode will be depleted. So, one of the key technologies has been that of an active air supply device which can feed sufficient air into the DMFC pack.

For portable application, the air supply device should be characterized by thin structure (several millimeters), substantial air flow (more than 100 ml for 1 W DMFC), low power consumption, and high efficiency and reliability. Recently, the PZT-actuated pump was developed for use in the biotechnology, chemistry, medicine, and engineering industries [2,3]. Compared with other actuation principles (such as electrostatic [4], magnetostriction [5], and shape memory alloy [6]), the piezoelectric actuation provides good reliability, energy efficiency, and moderated displacement. It provides a solution to the question of supplying air to the micro fuel cell. Several types of piezoelectric material including disk type, cantilever type, stack type, polymer type [7–10], etc. are used in pump actuators. Each type of the piezoelectric material has its characteristics. For example, the bimorph which is a kind of cantilever type

* Corresponding author. Tel.: +86 10 6279 6379; fax: +86 10 6277 1478.
E-mail address: yangxing@mail.tsinghua.edu.cn (X. Yang).

0924-4247/$ – see front matter © 2005 Elsevier B.V. All rights reserved.
doi:10.1016/j.sna.2005.12.021

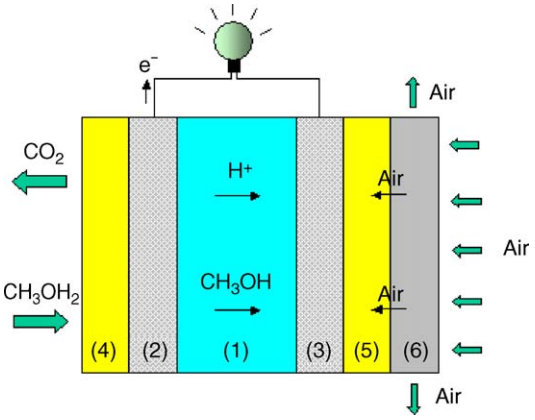

Fig. 1. The principle of DMFC and air supply to DMFC by air pump: (1) proton conducting membrane; (2 and 3) catalyst layer; (4) liquid diffusion electrode (anode); (5) air diffusion electrode (cathode); (6) air pump.

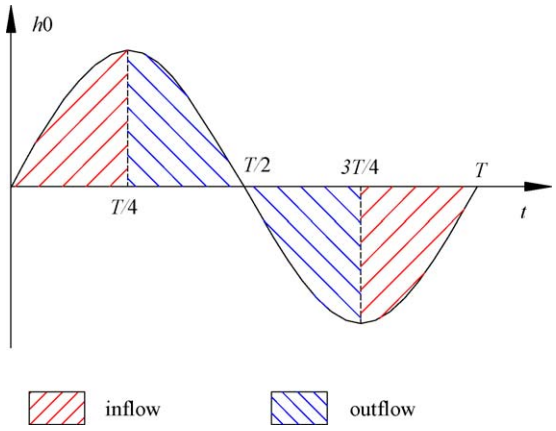

Fig. 3. The air flows in bottom cavity into one period; t and h_0 are time and vibration amplitude of the diaphragm.

piezoelectric material has large deformation and low drive voltage, but the output force is small. Large deformation is more important than output force in the application of pumping gas. Therefore, considered large deformation and thin structure, the bimorph actuator and diaphragm-type pump were used in this research, although few studies had reported on the large flow PZT-actuated structure for the gas pump and how it was used in air supply of micro fuel cells. In this paper, we introduce a gas pump with novel bimorphs actuation structure to feed air into the micro DMFC.

As shown in Fig. 1, when the air pump is working, the fresh air is sucked into the pump cavity through the topside of the pump. Then, the air passes through the air diffusion cathode's surface of the DMFC and flows out the cavity from the pump's side. Details about the micro diaphragm air pump will be presented in following sections.

2. Structure and working principle of the micro diaphragm air pump

Air pumps require a larger change in volume than liquid pumps since air can be compressed [11]. So, a diaphragm air pump whose actuation structure could produce a large volumetric ratio was presented.

As shown in Fig. 2, the diaphragm air pump consists of a cavity and an actuation structure. The actuation structure consists of two bimorphs and a diaphragm with an array of check valves (only one check valve is drawn in Fig. 2). When alternating voltage is applied, the bimorphs will vibrate and drive the diaphragm to move up and down. The diaphragm's amplitude is largest when the actuation structure is resonating [12]. Because the four sides of the diaphragm are not fixed, the diaphragm's motion is like a piston moving in a cylinder. Thus, a considerable change in volume is obtained that is suitable for pumping gases.

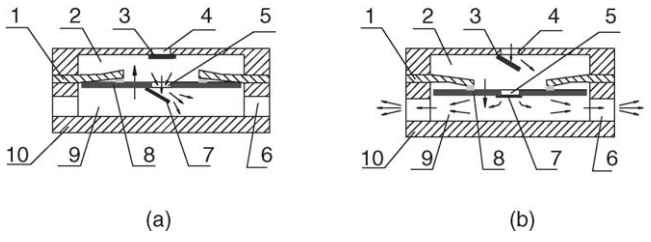

Fig. 2. Schematic diagram of diaphragm air pump. (a) The diaphragm moves upwards. (b) The diaphragm moves downwards: (1) bimorph; (2) top cavity; (3) check valve; (4) orifice on shell; (5) orifice on diaphragm; (6) vent; (7) check valve; (8) diaphragm; (9) bottom cavity; (10) pump's shell in contact with DMFC.

When the diaphragm is moving upwards (Fig. 2(a)), the air in the top cavity will flow into the bottom cavity. Although there is not a check valve in the vent (because it is difficult to reliably fabricate and work in this position), only a little air flows into the bottom cavity through the vent because the top shell is enclosed. When the diaphragm is moving downwards (Fig. 2(b)), the air in the bottom cavity will be pushed out through the vents and fresh external air will flow into the top cavity. Repeating in this way, the fresh air will continuously flow into the pump's bottom cavity and pass through the pump's bottom shell, which is in contact with the DMFC.

If the drive voltage is the sine wave, in one period T, the air flows into the pump's bottom cavity in [0, T/4] and [3T/4, T]. The air flows out the pump's bottom cavity in [T/4, 3T/4]. It is easy to see that the inflow is approximately equal to the outflow in one period, as shown in Fig. 3.

Maybe there will be a little leakage through the four sides of the diaphragm, but this is not important in its application to air supply of the micro fuel cell. Based on the principle above, a diaphragm air pump prototype with a cavity dimension of 60 mm × 16 mm × 2 mm was fabricated by precise manufacture. The material of the pump's shell was polymethyl methacrylate. The check valves were made of plastic film. The diaphragm with holes was fabricated by linear cutting and EDM machining out of a 100 μm thickness stainless steel sheet. There were five group check valves fabricated on the diaphragm and four check valve holes in one group. The diameter of the valves' holes was 1 mm. Fig. 4 shows the solid figure and photo of the diaphragm air pump's prototype, where the labels correspond to the ones in Fig. 2.

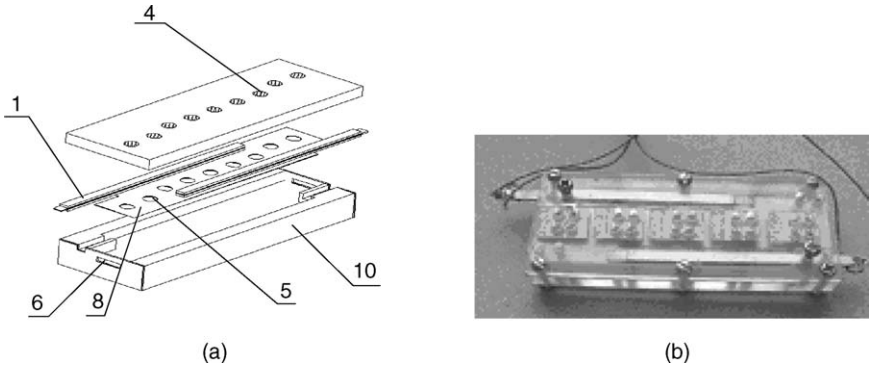

Fig. 4. (a) Solid figure and (b) photograph of diaphragm air pump's prototype.

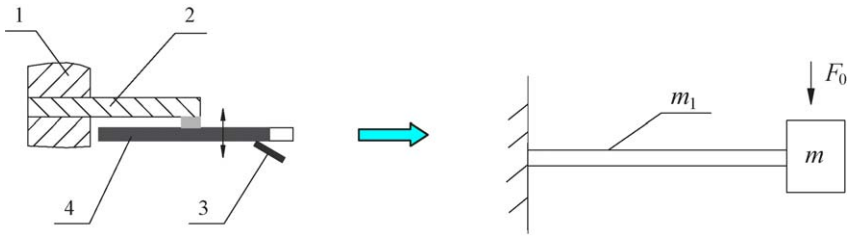

Fig. 5. Simplified diagram of actuation structure: (1) pump's shell; (2) bimorph; (3) half of the check valve; (4) half of the diaphragm.

3. Modeling

3.1. Natural frequency of actuation structure

Because of its symmetry, we could get one-half of the actuation structure to calculate. From Fig. 5, one-half of the actuation structure could be simplified as a cantilever (the equivalent of the bimorph) with a mass (the equivalent of the half of the diaphragm), where the cantilever is fixed at one end. The bimorph's drive force is equivalent to the external force (F_0) on the mass.

The first-order natural angular frequency ω_0 of the cantilever with a mass can be calculated by the Dunkerley Method [13]:

$$\frac{1}{\omega_0^2} = \frac{ml^3}{3EI} + \frac{m_1 l^3}{12.7EI}, \quad I = \frac{bt^3}{12} \tag{1}$$

where m and m_1 are equivalent masses of the bimorph and the half of the diaphragm, respectively; l, E, b and I are the cantilever's length, Young's modulus, width, and inertial moment. From Eq. (1), the first-order natural frequency f_0 of the actuation structure is obtained as follows:

$$f_0 = \frac{1}{2\pi}\sqrt{\frac{1}{(ml^3/3EI) + (m_1 l^3/12.7EI)}} \tag{2}$$

3.2. Amplitude of diaphragm

If only the first-order vibration is considered, the actuation structure in the pump can be further simplified to a single-degree-of-freedom system (Fig. 6).

When the bimorphs are driven by the sine wave voltage, assume the displacement from the diaphragm's equilibrium position is h, the half of the equivalent mass of the actuation structure is m_d, damping coefficient is c, equivalent stiffness is k, amplitude of equivalent piezoelectric force is F_0, the differential equation for describing the system vibration is [4]:

$$m_d h'' + ch' + kh = F_0 \sin 2\pi ft \tag{3}$$

assuming $h = h_0 \sin 2\pi ft$ (h_0 is vibration amplitude), and the damping ratio of the actuation structure is ζ. From Eq. (3), the amplitude is obtained as:

$$h_0 = \frac{|F_0/k|}{\sqrt{(1-(f^2/f_0^2))^2 + (2\zeta(f/f_0))^2}} \tag{4}$$

where l and t are the length and the thickness of the bimorph and d_{31} is the piezoelectric constant. When the voltage U is applied, the displacement at the end of the bimorph is [14]:

$$\delta = \left|\frac{F_0}{k}\right| = \frac{3l^2}{t^2} d_{31} U \tag{5}$$

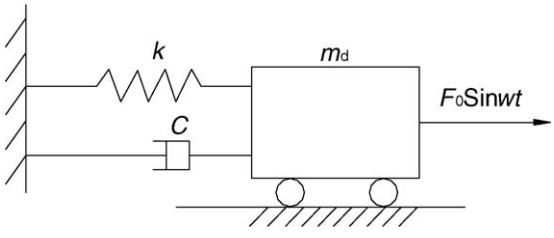

Fig. 6. Single-degree-of-freedom model of actuation structure.

Substituting the equation above into Eq. (4), the amplitude of the diaphragm is obtained as follows:

$$h_0 = \frac{|F_0/k|}{\sqrt{(1-(f^2/f_0^2))^2 + (2\zeta(f/f_0))^2}} = \frac{3l^2 d_{31} U}{t^2\sqrt{(1-(f^2/f_0^2))^2 + (2\zeta(f/f_0))^2}} \quad (6)$$

3.3. Flow rate in vent

As shown in Fig. 3, the air flow into the pump's bottom cavity is equal to the air flow out of the pump's bottom cavity in one period. So, we just calculate the flow rate in [T/4, 3T/4]. Because the Mach-number in the pump cavity is less than 0.3, the compression can be neglected.

Assume h_v is the distance between the diaphragm and pump cavity's bottom surface. It can be expressed as $h_v = h' + h_0 \sin 2\pi ft$, where h' is the original distance between the diaphragm and pump cavity's bottom surface. If the compression and the leakage are not considered, the instantaneous volume (V) of the pump's cavity in [T/4, 3T/4] is:

$$V = h_v BL = (h' + h_0 \sin 2\pi ft) BL \quad (7)$$

where L and B are the length and the width of the pump chamber. The change ratio of the instantaneous volume being equal to the instantaneous flow Q, we have:

$$Q = V' = 2\pi f BL h_0 \cos 2\pi ft \quad (8)$$

As we see, the pump's instantaneous flow also could be expressed as:

$$Q = 2Av \quad (9)$$

$$A = Bh = B(h' + h_0 \sin 2\pi ft) \quad (10)$$

where A and v are the instantaneous vent's cross-section area and the vent's flow velocity in pump cavity length direction (x-direction), respectively; from Eqs. (8), (9) and Eq. (10), we have:

$$v = \frac{Q}{2A} = \frac{h_0 L\pi f \cos 2\pi ft}{h' + h_0 \sin 2\pi f} \quad (11)$$

Thus, the mean flow velocity $\bar{v}$ is:

$$\bar{v} = \frac{\int_{(1/4)T}^{(3/4)T} v\,\mathrm{d}t}{T} = \frac{\pi f}{T}\int_{(1/4)T}^{(3/4)T} \frac{h_0 L \cos 2\pi ft}{h' + h_0 \sin 2\pi ft}\,\mathrm{d}t \quad (12)$$

Eq. (12) can be simplified to:

$$\bar{v} = \frac{L}{2T}\ln\frac{h' - h_0}{h' + h_0} \quad (13)$$

If we assume that ξ is the leakage factor, the mean flow velocity, taking leakage into consideration, is as follows:

$$\bar{v} = \xi\frac{L}{2T}\ln\frac{h' - h_0}{h' + h_0} \quad (14)$$

Substitute Eq. (6) and $f = 1/T$ into Eq. (14):

$$\bar{v} = \frac{Lf\xi}{2}\ln\frac{h't^2\sqrt{(1-(f^2/f_0^2))^2 + (2\zeta(f/f_0))^2} - 3l^2 d_{31} U}{h't^2\sqrt{(1-(f^2/f_0^2))^2 + (2\zeta(f/f_0))^2} + 3l^2 d_{31} U} \quad (15)$$

This is the expression of the diaphragm air pump's mean flow velocity, which is related to the amplitude and the frequency of the voltage, the pump's cavity length, the bimorph's parameters, etc.

4. Simulations

From the above models (Eqs. (2), (6) and (15)), simulation results for the first-order natural frequency, the vibration amplitude of the diaphragm and the flow velocity of the pump were obtained. Simulating parameters used are listed in Table 1.

The value of damping ratio (ζ) was obtained from experiments. It is difficult to determine the leakage factor (ξ) exactly. In this paper, we think ξ approximately depended on the ratio of the pump's width to length. It is about 0.196. According to calculations, the first-order natural frequency is about 124 Hz. The simulation curves representing frequency versus amplitude and flow velocity, when voltage is 20 V, are shown in Figs. 8 and 10. The simulation curve and experimental curve were drawn in one figure for the purpose of their convenient comparison.

The simulation results demonstrate that the mean flow velocity in the pump's vent is largest when resonating (about 124 Hz). The maximal mean flow velocity is about 0.184 m/s when the voltage is 20 V.

5. Experiments

5.1. Amplitude and flow rate

The vibration velocity of the diaphragm was measured by laser vibrometer (model number: CLV1000). Then, the amplitude was be obtained by integrating the velocity. The photo and the measured schematic diagram are shown in Fig. 7. The measured results are illustrated in Fig. 8.

It is difficult to measure the interior air flow velocity of the pump, for its size is very small (especially its thickness). It is seen that the pump's mean flow per minute can be calculated by

Table 1
Simulation parameters

l (m)	39×10^{-3}
t (m)	0.8×10^{-3}
E (GPa)	76.38
ζ	0.05
b (m)	2×10^{-3}
d_{31} (m/V)	-173×10^{-12}
L (m)	60×10^{-3}
B (m)	16×10^{-3}
U/V	20
ξ	0.196

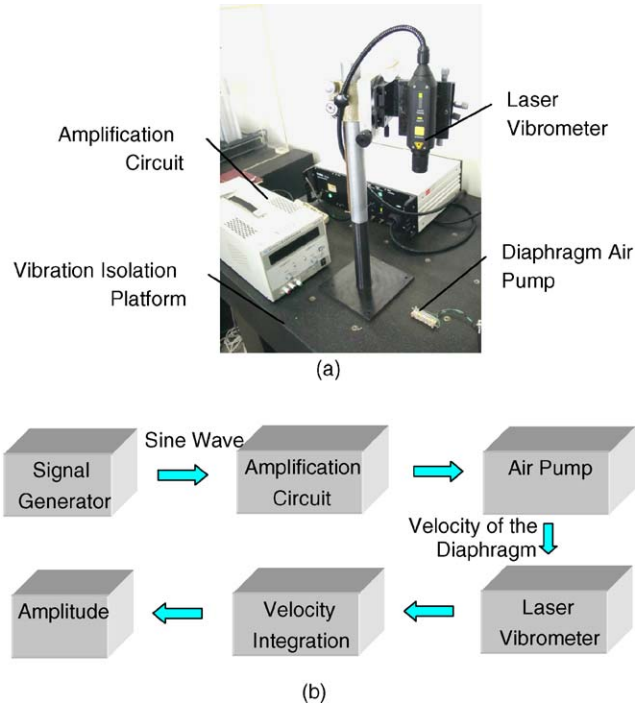

Fig. 7. (a) Photo and (b) schematic diagram of measuring the amplitude of the air pump's diaphragm by laser vibrometer.

the following formula:

$$\bar{Q} = 2 \times 60 \bar{v} \bar{A} \tag{16}$$

where $\bar{v}$ and $\bar{A}$ are the mean flow velocity in the pump vent and the vent's mean cross-section area, respectively. The mean air velocity in the vent (label 6 shown in Fig. 2) was measured by laser Doppler velocimeter (LDV). Fig. 9 is the photo of the experimental field.

The measured mean flow velocity in the pump's vent at different frequencies, when voltage is 20 V, is illustrated in Fig. 10.

Figs. 8 and 10 demonstrate that when drive voltage is 20 V, the mean flow velocity (in the pump's vent) and the amplitude

Fig. 9. Photo of measuring mean air velocity in vent by laser Doppler velocimeter.

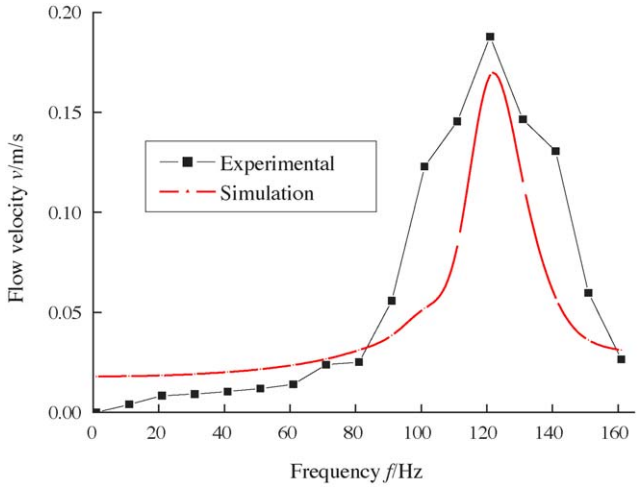

Fig. 10. Simulation curve and experimental curve of frequency vs. flow velocity.

of the diaphragm are maximal in the resonating state. They are 0.188 m/s and 0.00041 m, respectively. The value of $\bar{A}$ calculated is 3.78×10^{-6} m^2. From Eq. (16), the pump's mean flow rate is 85.3 ml/min. The experimental results basically agree with the simulation results, although there is a difference between measured value and calculated value. Analysis suggests the reason

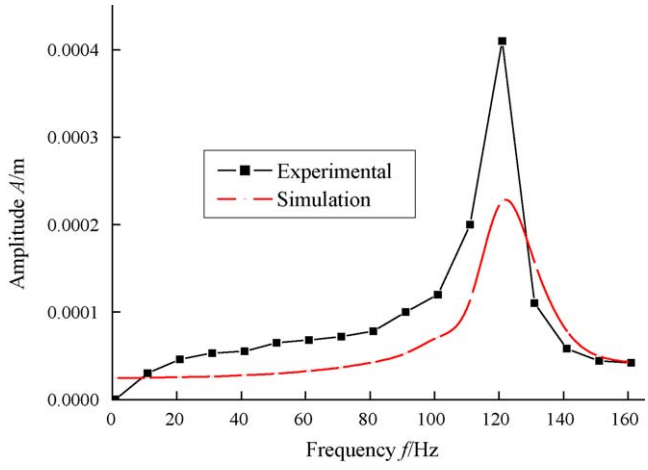

Fig. 8. Simulation curve and experimental curve of frequency vs. amplitude.

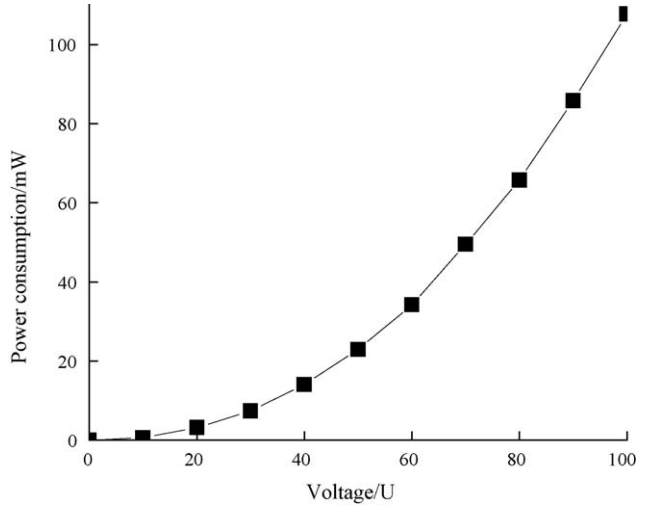

Fig. 11. Voltage vs. power consumption.

may be that the estimations of leakage factor and damping ratio are not exact enough.

5.2. Power consumption

The pump's power consumption was obtained by multiplying the current's effective value by the voltage's effective value. The results measured by ammeter are shown in Fig. 11.

The figure shows that the power consumption increases with the increase of drive voltage. The power consumption is about 3.18 mW at 20 V. Because the pump is actuated by PZT elements, the power consumption is very small.

6. Conclusions

In this study, a micro diaphragm PZT-actuated pump for the DMFC's air supply was presented numerically and experimentally. A novel large-displacement actuation structure was designed for the air pump, which utilized the bimorph's resonance. It was an effective way to greatly increase the volumetric ratio of the diaphragm pump.

The diaphragm pump has a simple and reliable structure. From experiments and simulation, the diaphragm air pump was shown to have good performance. With a voltage of 20 V, the air pump's flow rate is 85.3 ml/min in resonance and its power consumption is only 3.18 mW. Therefore, the diaphragm air pump proposed is suitable for air supply of the DMFC.

Acknowledgements

This work was supported by a grant from the Major State Basic Research Development Program of China (973-Program, G1999033106) and by a grant from the China Postdoctoral Science Foundation (No. 2003033125).

References

[1] K. Cowey, K.J. Green, G.O. Mepsted, R. Reeve, Portable and military fuel cells, Curr. Opin. Solid State Mater. Sci. 8 (2004) 367–371.
[2] D.S. Leea, J.S. Ko, Y.T. Kim, Bidirectional pumping properties of a peristaltic piezoelectric micropump with simple design and chemical resistance, Thin Solid Films 468 (2004) 285–290.
[3] L. Cao, S. Mantell, D. Polla, Design and simulation of an implantable medical drug delivery system using microelectromechanical systems technology, Sens. Actuators A 94 (2001) 117–125.
[4] R. Zengerle, M. Kluge, A. Richter, A bi-directional silicon micropump, Sens. Actuators A 50 (1995) 81–86.
[5] E. Quandt, K. Seemann, Magnetostrictive thin film microflow devices, in: Proceedings of the Microsystems Technology, vol. 96, Berlin, Germany, 1996, pp. 451–456.
[6] W.L. Benard, H. Kahn, A.H. Heuer, M.A. Huff, Thin-film shape memory alloy actuated micropumps, J. Microelectromech. Syst. 7 (1998) 245–251.
[7] M. Anjanappa, R. Angara, L. Si, Micro/MEMS actuators for microfluidic applications, in: Proceedings of ISSS 2005, International Conference on Smart Materials Structures and Systems, Bangalore, India, July 28–30, 2005, pp. SE64–SE71.
[8] M. Esashi, S. Shoji, A. Nakano, Normally closed microvalve and micropump fabricated on a silicon-wafer, Sens. Actuators 20 (1989) 163–169.
[9] A. Olsson, G. Stemme, E. Stemme, Valveless planar fluid pump with two pump chambers, Sens. Actuators A 47 (1995) 549–556.
[10] S.D. Deshpande, J. Kim, S.R. Yun, Studies on conducting polymer electroactive paper actuators: effect of humidity and electrode thickness, Smart Mater. Struct. 14 (2005) 876–880.
[11] T. Gerlach, Pumping gases by a silicon micro pump with dynamic passive valves, in: Proceedings of Transducers'97, Chicago, USA, June 16–19, 1997, pp. 357–360.
[12] J.H. Yoo, J.I. Hong, W. Cao, Piezoelectric ceramic bimorph coupled to thin metal plate as cooling fan for electronic devices, Sens. Actuators 79 (2000) 8–12.
[13] Z.W. Hu, Foundation of Engineering Vibration Analysis, first ed., Shanghai Jiaotong University Press, Shanghai, 1999, p. 75.
[14] J.G. Smits, S.I. Dalke, T.K. Cooney, The constituent equations of piezoelectric bimorph, Sens. Actuators A28 (1991) 41–61.

Biographies

Xing Yang graduated from Dalian University of Technology in 2002 with a PhD degree. He is a teacher in the Micro/Nano Technology Research Center at Tsinghua University. He has published more than 30 scientific papers and applied for 5 patents. His research interest is in the fields of MEMS, micro actuator, micro fluidic device, micro fuel cell and mechatronics.

Zhaoying Zhou graduated from the Department of Precision Instruments, Tsinghua University (Beijing, China), in 1961. He is a professor and Academic Committee Chairman in the Micro/Nano Technology Research Center at Tsinghua University. Prof. Zhou has published five technical books, and more than 200 scientific and technical papers. His research interest is in the fields of measurement, control and MEMS, and he is involved in three state key MEMS projects.

Hyejung Cho received her PhD from POSTECH in 1996. She is a member of the research staff in the MEMS Lab at the Samsung Advanced Institute of Technology, Korea. Her research fields include micro fuel cell, MEMS, etc.

Xiaobing Luo was born in 1974 and graduated from Tsinghua University with a PhD in 2002. He currently is a researcher in the MEMS Lab at the Samsung Advanced Institute of Technology, Korea. His research fields include micro fluidic device, MEMS, etc.